EARTHQUAKE ENGINEERING AND STRUCTURAL DYNAMICS
Earthquake Engng Struct. Dyn. 2001; **30**:59–80

Modified state–space procedures for pseudodynamic testing

Yen-Po Wang*,†, Chien-Liang Lee and Tzen-Hun Yo

Department of Civil Engineering, National Chiao-Tung University, 1001 Ta Hsueh Road, Hsinchu, Taiwan

SUMMARY

The existing on-line numerical integration algorithms are derived from the Newmark method, which is based on an approximation of derivatives in the differential equation. The state–space procedure (SSP), based on an interpolation of the discrete excitation signals for piecewise convolution integral, has been confirmed as more reliable than the Newmark method in terms of numerical accuracy and stability. In an attempt to enhance the pseudodynamic test, this study presents an on-line integration algorithm (referred to as the OS–SSP method) via an integration of the state–space procedure with Nakashima's operator-splitting concept. Numerical stability and accuracy assessment of the proposed algorithm in addition to the explicit Newmark method and the OS method were investigated via an eigenvalue, frequency-domain and time-domain analysis. Of the on-line integration algorithms investigated, the OS–SSP method is demonstrated as the most accurate method with an acceptable stability (although not unconditionally stable) characteristic. Therefore, the OS–SSP method is the most desirable method for pseudodynamic testing if the numerical stability criterion ($\Delta t/T \leqslant 0.5$) is ensured for every vibration mode involved. Copyright © 2001 John Wiley & Sons, Ltd.

KEY WORDS: state space; pseudodynamic testing; earthquake; on-line integration

1. INTRODUCTION

The dynamic testing of large-scale structures continues to play a significant role in earthquake engineering research. Although the shaking table test is recognized as the most direct means for earthquake simulation, the pseudodynamic test has been an effective and widely accepted practice since the initial studies by Takanashi *et al.* [1], Shing and Mahin [2] and Mahin and Shing [3]. In a pseudodynamic test, the reaction forces of the tested structure or its components are directly measured, and fed back on-line for earthquake response analysis via numerical integration. A pseudodynamic test, requiring a quasi-static loading actuator, allows for the testing of larger-scale structures than those permitted by a shaking table test. Additionally, the sub-structuring

* Correspondence to: Yen-Po Wang, Department of Civil Engineering, National Chiao-Tung University, 1001 Ta Hsueh Road, Hsinchu, Taiwan.
† E-mail: ypwang@cc.nctu.edu.tw.
Contract/grant sponsor: National Science Council of the Republic of China; Contract/grant number: NSC 87-2211-E009-028.

Received 27 April 1999
Revised 28 April 2000
Accepted 4 May 2000

technique further reduces experiment cost. Clearly, the pseudodynamic test is more favourable for tests requiring full-scale implementation.

The pseudodynamic test is an approximate means of simulating quasi-static dynamic structural responses. One major difficulty in pseudodynamic testing is that results are very sensitive to experimental errors. The error resources of a pseudodynamic test are primarily executing errors introduced during the loading process, and numerical errors introduced during the direct integration process [4–6]. In order to avoid complications that may result from iterative procedures during pseudodynamic testing, the dynamic integration algorithms employed are normally explicitly represented (for example, the explicit Newmark method). However, the explicit-type algorithms do not preserve the desired characteristics of stability and accuracy. To overcome this difficulty, Thewalt and Mahin [7] presented an unconditionally stable implicit integration scheme via the introduction of an analog electrical device without iterative procedures for displacement correction. Nakashima *et al.* [8] presented the operator-splitting (OS) method by dividing the displacement term into the implicit and explicit parts. A pseudodynamic test corrects displacement via a one-step predictor–corrector iterative process without the employment of an extra electrical device (as required by Thewalt and Mahin [7]). Additionally, if an appropriate parameter is chosen the OS method is unconditionally stable, as verified by Nakashima *et al.* [8]. This method is particularly advantageous in testing structures with inelastic behaviours.

The aforementioned numerical integration algorithms are derived from the Newmark method, which is based on the approximation of derivatives in the differential equation. However, the state-space procedure (SSP) [9, 10] (based on the interpolation of the discrete excitation signals for piecewise convolution integral) is more reliable than the Newmark method in terms of both numerical accuracy and stability. In an attempt to enhance the pseudodynamic test, an SSP-based integration algorithm (referred to as the OS–SSP method) is presented via an integration of Nakashima's [8] operator-splitting concept with the state-space procedure. Although the original state-space procedure is unconditionally stable, its derivative (i.e. OS–SSP) does not preserve the desired characteristics of numerical stability, requiring further investigation. Accuracy assessment of the proposed algorithms in addition to the explicit Newmark method and the OS method is investigated via an eigenvalue, frequency- and the time-domain analysis of both linear and non-linear structures. Of the on-line integration algorithms investigated, the OS–SSP method is illustrated as the most accurate method with acceptable stability (although not unconditionally stable) characteristic. Therefore, the OS–SSP method is the most desirable method for pseudodynamic testing if the numerical stability criterion ($\Delta t/T \leqslant 0.5$) is ensured for every vibration mode involved.

2. DERIVATION OF DIFFERENCE EQUATIONS

When an n degree-of-freedom (DOF) structure is subjected to earthquake loads $w(t)$, its equation of motion can be expressed as

$$\mathbf{M}\ddot{\mathbf{x}}(t) + \mathbf{C}\dot{\mathbf{x}}(t) + \mathbf{K}\mathbf{x}(t) = \hat{\mathbf{E}}w(t) \tag{1}$$

where $\mathbf{x}(t)$ is an $n \times 1$ displacement vector, $\mathbf{M}$ is an $n \times n$ mass matrix, $\mathbf{C}$ is an $n \times n$ damping matrix, $\mathbf{K}$ is an $n \times n$ stiffness matrix, and $\hat{\mathbf{E}}$ is an $n \times 1$ earthquake-loading vector. In pseudodynamic tests, the restoring force of the structure is the reaction force measured when the structure is forced to the estimated position $\mathbf{x}(t)$ by the hydraulic actuator. Therefore, the term $\mathbf{K}\mathbf{x}(t)$, in

Equation (1) is replaced by the restoring force, $\mathbf{R}(t)$, as

$$\mathbf{M}\ddot{\mathbf{x}}(t) + \mathbf{C}\dot{\mathbf{x}}(t) + \mathbf{R}(t) = \hat{\mathbf{E}}w(t) \tag{2}$$

regardless of linear or non-linear systems.

2.1. Explicit Newmark method

The basic equations of the Newmark method [11] are generally formulated as

$$\mathbf{M}\ddot{\mathbf{x}}_{k+1} + \mathbf{C}\dot{\mathbf{x}}_{k+1} + \mathbf{R}_{k+1} = \hat{\mathbf{E}}w_{k+1} \tag{3}$$

$$\mathbf{x}_{k+1} = \mathbf{x}_k + \Delta t\dot{\mathbf{x}}_k + \Delta t^2[(\tfrac{1}{2} - \alpha)\ddot{\mathbf{x}}_k + \alpha\ddot{\mathbf{x}}_{k+1}] \tag{4}$$

$$\dot{\mathbf{x}}_{k+1} = \dot{\mathbf{x}}_k + \Delta t[(1 - \delta)\ddot{\mathbf{x}}_k + \delta\ddot{\mathbf{x}}_{k+1}] \tag{5}$$

where Δt is the integration time interval, the subscript k indicates values at time equal to $k\Delta t$ and α and δ are parameters characterizing the approximation strategy. This numerical scheme can be directly implemented for pseudodynamic testing by setting parameter α to be zero. Equation (4) is then simplified as

$$\mathbf{x}_{k+1} = \mathbf{x}_k + \Delta t\dot{\mathbf{x}}_k + \frac{\Delta t^2}{2}\ddot{\mathbf{x}}_k \tag{6}$$

in an explicit manner. With $\mathbf{x}_{k+1}$ calculated, the structure is then repositioned accordingly.

For linear structures, the restoring force $\mathbf{R}_{k+1} = \mathbf{K}x_{k+1}$. The structural response represented by Equations (3), (5) and (6) can be concisely expressed in a recursive matrix form as

$$\mathbf{z}_{k+1} = \mathbf{A}\mathbf{z}_k + \mathbf{E}w_{k+1} \tag{7}$$

where

$$\mathbf{z}_k = \begin{bmatrix} \mathbf{x}_k \\ \Delta t\dot{\mathbf{x}}_k \\ \Delta t^2\ddot{\mathbf{x}}_k \end{bmatrix}$$

is a $3n \times 1$ structural response vector,

$$\mathbf{A} = \begin{bmatrix} \mathbf{I} & \mathbf{I} & \tfrac{1}{2}\mathbf{I} \\ -\delta\Delta t^2\hat{\mathbf{M}}^{-1}\mathbf{K} & \mathbf{I} - \delta\Delta t\hat{\mathbf{M}}^{-1}\mathbf{C} - \delta\Delta t^2\hat{\mathbf{M}}^{-1}\mathbf{K} & (1-\delta)(\mathbf{I} - \delta\Delta t\hat{\mathbf{M}}^{-1}\mathbf{C}) - \dfrac{\delta\Delta t^2}{2}\hat{\mathbf{M}}^{-1}\mathbf{K} \\ -\Delta t^2\hat{\mathbf{M}}^{-1}\mathbf{K} & -\Delta t\hat{\mathbf{M}}^{-1}\mathbf{C} - \Delta t^2\hat{\mathbf{M}}^{-1}\mathbf{K} & -\hat{\mathbf{M}}^{-1}\mathbf{C}\Delta t(1-\delta) - \dfrac{\Delta t^2}{2}\hat{\mathbf{M}}^{-1}\mathbf{K} \end{bmatrix}$$

is a $3n \times 3n$ effective system matrix,

$$\mathbf{E} = \begin{bmatrix} \mathbf{0} \\ \delta\Delta t^2\hat{\mathbf{M}}^{-1}\hat{\mathbf{E}} \\ \Delta t^2\hat{\mathbf{M}}^{-1}\hat{\mathbf{E}} \end{bmatrix}$$

is a $3n \times 1$ effective load vector and $\hat{\mathbf{M}} = \mathbf{M} + \mathbf{C}\delta\Delta t$ is an $n \times n$ effective mass matrix.

Without loss of generality, a single-degree-of-freedom (SDOF) structure is considered for stability and accuracy assessment. Therefore, the effective system matrix **A** and the effective load vector **E** are reduced, respectively, as

$$\mathbf{A} = \begin{bmatrix} 1 & 1 & \frac{1}{2} \\ -\delta\kappa & 1-\delta\beta-\delta\kappa & (1-\delta)(1-\delta\beta)-\dfrac{\delta\kappa}{2} \\ -\kappa & -(\beta+\kappa) & -\beta(1-\delta)-\dfrac{\kappa}{2} \end{bmatrix} \quad \text{and} \quad \mathbf{E} = \frac{1}{\omega_0^2}\begin{bmatrix} 0 \\ -\delta\kappa \\ -\kappa \end{bmatrix}$$

where $\beta = 2\zeta\omega_0\Delta t/(1+2\zeta\omega_0\delta\Delta t)$, $\kappa = \omega_0^2\Delta t^2/(1+2\zeta\omega_0\delta\Delta t)$ ω_0 and ζ are the natural frequency and damping ratio of the structure, respectively. β, κ and **A** are dimensionless favorable for numerical stability assessment.

2.2. *Operator-splitting method (OS)*

The operator-splitting method proposed by Nakashima *et al.* [8] is derived under the framework of Newmark method. The restoring force **R** in the equation of motion (2) is divided into implicit linear force $\mathbf{R}^{\mathrm{I}} = \mathbf{K}^{\mathrm{I}}\mathbf{x}$ and explicit non-linear corrective force $\mathbf{R}^{E}(\tilde{\mathbf{x}})$, i.e.

$$\mathbf{M}\ddot{\mathbf{x}}_{k+1} + \mathbf{C}\dot{\mathbf{x}}_{k+1} + \mathbf{K}^{\mathrm{I}}\mathbf{x}_{k+1} + \mathbf{R}^{\mathrm{E}}_{k+1} = \hat{\mathbf{E}}w_{k+1} \tag{8}$$

where $\mathbf{K}^{\mathrm{I}}$ is the initial stiffness of the structure, $\mathbf{R}^{\mathrm{E}}_{k+1} = \mathbf{R}_{k+1} - \mathbf{K}^{\mathrm{I}}\tilde{\mathbf{x}}_{k+1}$with $\tilde{\mathbf{x}}_{k+1}$being the predicted displacement of the $(k+1)$th time instant defined as

$$\tilde{\mathbf{x}}_{k+1} = \mathbf{x}_k + \Delta t\dot{\mathbf{x}}_k + (\tfrac{1}{2}-\alpha)\Delta t^2\ddot{\mathbf{x}}_k \tag{9}$$

which is the explicit part of Equation (3). During each step of the testing, the structure is positioned according to $\tilde{\mathbf{x}}_{k+1}$ estimated by Equation (9) and the restoring force $\mathbf{R}_{k+1}$ is measured. The velocity and acceleration responses of the structure are in turn estimated from Equations (4), (5) and (8) and the structure's displacement at time instant $k+1$ is then modified as

$$\mathbf{x}_{k+1} = \tilde{\mathbf{x}}_{k+1} + \alpha\Delta t^2\ddot{\mathbf{x}}_{k+1} \tag{10}$$

After elaborating the above-mentioned substitutions, the difference equation can be constructed as

$$\mathbf{z}_{k+1} = \mathbf{A}z_k + \mathbf{E}w_{k+1} + \mathbf{B}R^{\mathrm{E}}_{k+1} \tag{11}$$

where

$$\mathbf{A} = \begin{bmatrix} \mathbf{I}-\alpha\Delta t^2\hat{\mathbf{M}}^{-1}\mathbf{K}^{\mathrm{I}} & \mathbf{I}-\alpha\Delta t(\hat{\mathbf{M}}^{-1}\mathbf{C}+\Delta t\hat{\mathbf{M}}^{-1}\mathbf{K}^{\mathrm{I}}) & (\frac{1}{2}-\alpha)\mathbf{I}-\alpha\Delta t[(1-\delta)\hat{\mathbf{M}}^{-1}\mathbf{C}+(\frac{1}{2}-\alpha)\Delta t\hat{\mathbf{M}}^{-1}\mathbf{K}^{\mathrm{I}}] \\ -\delta\Delta t^2\hat{\mathbf{M}}^{-1}\mathbf{K}^{\mathrm{I}} & \mathbf{I}-\delta\Delta t\hat{\mathbf{M}}^{-1}\mathbf{C}-\delta\Delta t^2\hat{\mathbf{M}}^{-1}\mathbf{K}^{\mathrm{I}} & (1-\delta)(\mathbf{I}-\delta\Delta t\hat{\mathbf{M}}^{-1}\mathbf{C})-\delta(\frac{1}{2}-\alpha)\Delta t^2\hat{\mathbf{M}}^{-1}\mathbf{K}^{\mathrm{I}} \\ -\Delta t^2\hat{\mathbf{M}}^{-1}\mathbf{K}^{\mathrm{I}} & -\Delta t(\hat{\mathbf{M}}^{-1}\mathbf{C}+\Delta t\hat{\mathbf{M}}^{-1}\mathbf{K}^{\mathrm{I}}) & -\Delta t[(1-\delta)\hat{\mathbf{M}}^{-1}\mathbf{C}+(\frac{1}{2}-\alpha)\Delta t\hat{\mathbf{M}}^{-1}\mathbf{K}^{\mathrm{I}}] \end{bmatrix}$$

is the $3n\times 3n$ effective system matrix,

$$\mathbf{E} = \begin{bmatrix} \alpha\Delta t^2\hat{\mathbf{M}}^{-1}\hat{\mathbf{E}} \\ \delta\Delta t^2\hat{\mathbf{M}}^{-1}\hat{\mathbf{E}} \\ \Delta t^2\hat{\mathbf{M}}^{-1}\hat{\mathbf{E}} \end{bmatrix}$$

is the $3n \times 1$ effective load vector,

$$\mathbf{B} = \begin{bmatrix} -\alpha\Delta t^2 \hat{\mathbf{M}}^{-1} \\ -\delta\Delta t^2 \hat{\mathbf{M}}^{-1} \\ -\Delta t^2 \hat{\mathbf{M}}^{-1} \end{bmatrix}$$

is the $3n \times n$ effective correcting matrix, and $\hat{\mathbf{M}} = \mathbf{M} + \delta\Delta t\mathbf{C} + \alpha\Delta t^2\mathbf{K}^{\mathrm{I}}$ is the $n \times n$ effective mass matrix.

Without loss of generality, the stability and accuracy of the numerical method is investigated by considering a SDOF structure. Defining parameter θ to be the ratio between the initial stiffness and the actual stiffness (i.e. the instantaneous tangent stiffness) of the structure, that is

$$\mathbf{K}^{\mathrm{I}} = \theta\mathbf{K} \tag{12}$$

and the corrective force $\mathbf{R}^E_{k+1} = (1-\theta)\mathbf{K}\tilde{\mathbf{x}}_{k+1}$, the effective system matrix $\mathbf{A}$ and the effective load matrix $\mathbf{E}$ are simplified, respectively, as

$$\mathbf{A} = \begin{bmatrix} 1-\alpha\kappa & 1-\alpha\beta-\alpha\kappa & (\frac{1}{2}-\alpha)-\alpha\beta(1-\delta)-\alpha(\frac{1}{2}-\alpha)\kappa \\ -\delta\kappa & 1-\delta\beta-\delta\kappa & (1-\delta)(1-\delta\beta)-\delta(\frac{1}{2}-\alpha)\kappa \\ -\kappa & -(\beta+\kappa) & -(1-\delta)\beta-(\frac{1}{2}-\alpha)\kappa \end{bmatrix} \quad \text{and} \quad \mathbf{E} = \frac{-1}{\omega_0^2}\begin{bmatrix} \alpha\kappa \\ \delta\kappa \\ \kappa \end{bmatrix}$$

where

$$\beta = \frac{2\zeta\omega_0\Delta t}{1+2\zeta\omega_0\delta\Delta t+\theta\alpha\omega_0^2\Delta t^2} \quad \text{and} \quad \kappa = \frac{\omega_0^2\Delta t^2}{1+2\zeta\omega_0\delta\Delta t+\theta\alpha\omega_0^2\Delta t^2}$$

are again dimensionless.

2.3. Operator–splitting state-space procedure (OS–SSP)

The equation of motion (2) is reformulated in a state-space form, leading to a first-order differential equation as

$$\dot{\mathbf{Z}}(t) = \mathbf{A}_{\mathrm{C}}\mathbf{Z}(t) + \mathbf{E}_{\mathrm{C}}w(t) + \mathbf{B}_{\mathrm{C}}\mathbf{R}(t) \tag{13}$$

where

$$\mathbf{Z}(t) = \begin{bmatrix} \mathbf{x}(t) \\ \dot{\mathbf{x}}(t) \end{bmatrix}$$

is a $2n \times 1$ continuous-time state vector,

$$\mathbf{A}_{\mathrm{C}} = \begin{bmatrix} \mathbf{0} & \mathbf{I} \\ \mathbf{0} & -\mathbf{M}^{-1}\mathbf{C} \end{bmatrix}$$

is a $2n \times 2n$ continuous-time system matrix,

$$\mathbf{E}_{\mathrm{C}} = \begin{bmatrix} \mathbf{0} \\ \mathbf{M}^{-1}\hat{\mathbf{E}} \end{bmatrix}$$

is a $2n \times 1$ continuous-time load vector, and

$$\mathbf{B}_{\mathrm{C}} = \begin{bmatrix} \mathbf{0} \\ -\mathbf{M}^{-1} \end{bmatrix}$$

is a $2n \times n$ continuous-time correcting force matrix.

Taking a Laplace transformation of Equation (13), it gives

$$\mathbf{Z}(s) = \mathbf{H}(s)\mathbf{Z}(t_0) + \mathbf{H}(s)\mathbf{G}(s) \tag{14}$$

where $\mathbf{Z}(t_0)$ denotes the initial conditions of the state at $t = t_0$, and

$$\mathbf{H}(s) = (s\,\mathbf{I} - \mathbf{A}_{\mathrm{C}})^{-1} \tag{15a}$$

$$\mathbf{G}(s) = \mathbf{E}_{\mathrm{C}}\mathbf{w}(s) + \mathbf{B}_{\mathrm{C}}\mathbf{R}(s) \tag{15b}$$

The solution of Equation (13) is then obtained by taking an inverse Laplace transformation of Equation (14) back to the time domain, giving

$$\mathbf{Z}(t) = \mathrm{e}^{\mathbf{A}_{\mathrm{C}}(t-t_0)}\mathbf{Z}(t_0) + \int_{t_0}^{t} \mathrm{e}^{\mathbf{A}_{\mathrm{C}}(t-\tau)}[\mathbf{E}_{\mathrm{C}}w(\tau) + \mathbf{B}_{\mathrm{C}}\mathbf{R}(\tau)]\,\mathrm{d}\tau \tag{16}$$

The external load $w(\tau)$ and the restoring force $\mathbf{R}(\tau)$ are recorded in the form of digital signals. It is reasonable to assume that the external load and the restoring force are linear between two consecutive sampling instants, that is

$$w(\tau) = \frac{(k+1)\Delta t - \tau}{\Delta t} w(k\Delta t) + \frac{\tau - k\Delta t}{\Delta t} w((k+1)\Delta t), \quad k\Delta t \leqslant \tau \leqslant (k+1)\Delta t \tag{17a}$$

$$\mathbf{R}(\tau) = \frac{(k+1)\Delta t - \tau}{\Delta t} \mathbf{R}(k\Delta t) + \frac{\tau - k\Delta t}{\Delta t} \mathbf{R}((k+1)\Delta t), \quad k\Delta t \leqslant \tau \leqslant (k+1)\Delta t \tag{17b}$$

When $t = (k+1)\Delta t$ and $t_0 = k\Delta t$ are assigned, from Equation (16), the analytical solution to the continuous-time state equation (13) is a difference equation as

$$\mathbf{Z}_{k+1} = \mathbf{A}_{\mathrm{D}}\mathbf{Z}_k + \mathbf{E}_0 w_k + \mathbf{E}_1 w_{k+1} + \mathbf{B}_0\mathbf{R}_k + \mathbf{B}_1\mathbf{R}_{k+1} \tag{18}$$

where $\mathbf{A}_{\mathrm{D}} = \mathrm{e}^{\mathbf{A}_{\mathrm{C}}\Delta t}$ is a $2n \times 2n$ discrete-time system matrix, which can be represented in the form of the Taylor series expansion as

$$\mathbf{A}_{\mathrm{D}} = \mathbf{I} + \mathbf{A}_{\mathrm{C}}\Delta t + \mathbf{A}_{\mathrm{C}}^2 \frac{\Delta t^2}{2!} + \cdots + \mathbf{A}_{\mathrm{C}}^n \frac{\Delta t^n}{n!} + \cdots$$

$$\mathbf{E}_0 = \left[\mathbf{A}_{\mathrm{C}}^{-1}\mathbf{A}_{\mathrm{D}} + \frac{1}{\Delta t}\mathbf{A}_{\mathrm{C}}^{-2}(\mathbf{I} - \mathbf{A}_{\mathrm{D}})\right]\mathbf{E}_{\mathrm{C}} \tag{19}$$

is a $2n \times 1$ load matrix of current time-step,

$$\mathbf{E}_1 = \left[-\mathbf{A}_C^{-1} + \frac{1}{\Delta t}\mathbf{A}_C^{-2}(\mathbf{A}_D - \mathbf{I}) \right] \mathbf{E}_C$$

is a $2n \times 1$ load matrix of next time-step,

$$\mathbf{B}_0 = \left[\mathbf{A}_C^{-1}\mathbf{A}_D + \frac{1}{\Delta t}\mathbf{A}_C^{-2}(\mathbf{I} - \mathbf{A}_D) \right] \mathbf{B}_C$$

is a $2n \times n$ correcting force matrix of current time-step, and

$$\mathbf{B}_1 = \left[-\mathbf{A}_C^{-1} + \frac{1}{\Delta t}\mathbf{A}_C^{-2}(\mathbf{A}_D - \mathbf{I}) \right] \mathbf{B}_C$$

is a $2n \times n$ correcting force matrix of next time-step.

Adopting the concept of operator-splitting, the restoring force, $\mathbf{R}$, in Equation (2) is divided into the implicit linear force $\mathbf{R}^I = \mathbf{K}^I\mathbf{x}$ and the explicit non-linear corrective force $\mathbf{R}^E(\tilde{\mathbf{x}})$, and the equation of motion can be reformulated as

$$\mathbf{M}\ddot{\mathbf{x}}(t) + \mathbf{C}\dot{\mathbf{x}}(t) + \mathbf{K}^I\mathbf{x}(t) + \mathbf{R}^E(\tilde{\mathbf{x}}) = \hat{\mathbf{E}}w(t) \tag{20}$$

and its state-space form counterpart becomes

$$\dot{\mathbf{Z}} = \mathbf{A}_C\mathbf{Z}(t) + \mathbf{E}_C w(t) + \mathbf{B}_C\mathbf{R}^E(t) \tag{21}$$

where

$$\mathbf{A}_C = \begin{bmatrix} \mathbf{0} & \mathbf{I} \\ -\mathbf{M}^{-1}\mathbf{K}^I & -\mathbf{M}^{-1}\mathbf{C} \end{bmatrix}$$

is a $2n \times 2n$ continuous-time system matrix.

The discrete-time state equation of Equation (21) is

$$\mathbf{Z}_{k+1} = \mathbf{A}_D\mathbf{Z}_k + \mathbf{E}_0 w_k + \mathbf{E}_1 w_{k+1} + \mathbf{B}_0\mathbf{R}_k^E + \mathbf{B}_1\mathbf{R}_{k+1}^E \tag{22}$$

where $\mathbf{A}_D, \mathbf{E}_0, \mathbf{E}_1, \mathbf{B}_0$ and $\mathbf{B}_1$ are as defined earlier.

During each step of the pseudodynamic testing, the corrective restoring force $\mathbf{R}_{k+1}^E = \mathbf{R}_{k+1} - \mathbf{K}^I\mathbf{x}_{k+1}$ at time instant $k+1$ is determined with $\mathbf{R}_{k+1}$ measured when the structure is displaced by $\mathbf{x}_{k+1} = \mathbf{D}Z_{k+1}$ where $D = [\mathbf{I} \quad 0]$. According to Equation (22), however, $\mathbf{Z}_{k+1}$ is a function of $\mathbf{R}_{k+1}^E$. Therefore, the solution requires an iterative process. To avoid the complication caused by an iterative process, the explicit part of the state in Equation (22) is considered as the predictor, that is

$$\tilde{\mathbf{Z}}_{k+1} = \mathbf{A}_D\mathbf{Z}_k + \mathbf{E_0} w_k + \mathbf{E}_1 w_{k+1} + \mathbf{B_0}\mathbf{R}_k^E \tag{23}$$

The predicted structural displacement, $\tilde{\mathbf{x}}_{k+1}$, is then calculated as

$$\tilde{\mathbf{x}}_{k+1} = \mathbf{D}\tilde{\mathbf{Z}}_{k+1} \tag{24}$$

$\mathbf{R}_{k+1}$ is measured as soon as the structure is moved to the target position and the corrective force $\mathbf{R}_{k+1}^E = \mathbf{R}_{k+1} - \mathbf{K}^I\tilde{\mathbf{x}}_{k+1}$ can be estimated which in turn is substituted into Equation (22) for $\mathbf{Z}_{k+1}$.

For linear structures, the corrective restoring force $\mathbf{R}_{k+1}^{\mathrm{E}}$ can be expressed as

$$\mathbf{R}_{k+1}^{\mathrm{E}} = (\mathbf{K} - \mathbf{K}^{\mathrm{I}})\mathbf{D}\tilde{\mathbf{Z}}_{k+1} \tag{25}$$

Notably, Equation (25) is also valid for time k, that is, $\mathbf{R}_{k}^{\mathrm{E}} = (\mathbf{K} - \mathbf{K}^{\mathrm{I}})\mathbf{D}\tilde{\mathbf{Z}}_{k}$. Substituting $\mathbf{R}_{k}^{\mathrm{E}}$ into Equation (23) gives

$$\tilde{\mathbf{Z}}_{k+1} = \mathbf{A}_{\mathrm{D}}\mathbf{Z}_k + \mathbf{E}_0 w_k + \mathbf{E}_1 w_{k+1} + \mathbf{B}_0(\mathbf{K} - \mathbf{K}^{\mathrm{I}})\mathbf{D}\tilde{\mathbf{Z}}_k \tag{26}$$

Further substitution of Equations (25) and (26) into Equation (22) leads to

$$\begin{aligned}\mathbf{Z}_{k+1} = {} & [\mathbf{I} + \mathbf{B}_1(\mathbf{K} - \mathbf{K}^{\mathrm{I}})\mathbf{D}]\mathbf{A}_{\mathrm{D}}\mathbf{Z}_k + [\mathbf{I} + \mathbf{B}_1(\mathbf{K} - \mathbf{K}^{\mathrm{I}})\mathbf{D}]\mathbf{B}_0(\mathbf{K} - \mathbf{K}^{\mathrm{I}})\tilde{\mathbf{x}}_k \\ & + [\mathbf{I} + \mathbf{B}_1(\mathbf{K} - \mathbf{K}^{\mathrm{I}})\mathbf{D}]\mathbf{E}_1 w_{k+1} + [\mathbf{I} + \mathbf{B}_1(\mathbf{K} - \mathbf{K}^{\mathrm{I}})\mathbf{D}]\mathbf{E}_0 w_k\end{aligned} \tag{27}$$

Defining the extended state vector

$$\bar{\mathbf{z}}_k = \begin{bmatrix} \mathbf{Z}_k \\ \tilde{\mathbf{x}}_k \end{bmatrix},$$

then from Equations (24), (26) and (27), the extended state equation is obtained as

$$\bar{\mathbf{z}}_{k+1} = \mathbf{A}\bar{\mathbf{z}}_k + \bar{\mathbf{E}}_0 w_k + \bar{\mathbf{E}}_1 w_{k+1} \tag{28}$$

where

$$\mathbf{A} = \begin{bmatrix} [\mathbf{I} + \mathbf{B}_1(\mathbf{K} - \mathbf{K}^{\mathrm{I}})\mathbf{D}]\mathbf{A}_{\mathrm{D}} & [\mathbf{I} + \mathbf{B}_1(\mathbf{K} - \mathbf{K}^{\mathrm{I}})\mathbf{D}]\mathbf{B}_0(\mathbf{K} - \mathbf{K}^{\mathrm{I}}) \\ \mathbf{D}\mathbf{A}_{\mathrm{D}} & \mathbf{D}\mathbf{B}_0(\mathbf{K} - \mathbf{K}^{\mathrm{I}}) \end{bmatrix}$$

is a $3n \times 3n$ effective system matrix,

$$\bar{\mathbf{E}}_1 = \begin{bmatrix} [\mathbf{I} + \mathbf{B}_1(\mathbf{K} - \mathbf{K}^{\mathrm{I}})\mathbf{D}]\mathbf{E}_1 \\ \mathbf{D}\mathbf{E}_1 \end{bmatrix} \quad \text{and} \quad \bar{\mathbf{E}}_0 = \begin{bmatrix} [\mathbf{I} + \mathbf{B}_1(\mathbf{K} - \mathbf{K}^{\mathrm{I}})\mathbf{D}]\mathbf{E}_0 \\ \mathbf{D}\mathbf{E}_0 \end{bmatrix}.$$

3. STABILITY ANALYSES OF NUMERICAL METHODS

For SDOF systems, the effective system matrix

$$\mathbf{A} = \begin{bmatrix} A_{11} & A_{12} & A_{13} \\ A_{21} & A_{22} & A_{23} \\ A_{31} & A_{32} & A_{33} \end{bmatrix}$$

is a 3×3 matrix. The characteristic equation of the system matrix can be expressed as

$$F(\gamma) = \gamma^3 - a_2\gamma^2 + a_1\gamma - a_0 = 0 \tag{29}$$

where

$$a_0 = \gamma_1\gamma_2\gamma_3 = \begin{vmatrix} A_{11} & A_{12} & A_{13} \\ A_{21} & A_{22} & A_{23} \\ A_{31} & A_{32} & A_{33} \end{vmatrix}$$

$$a_1 = \gamma_1\gamma_2 + \gamma_2\gamma_3 + \gamma_3\gamma_1$$

$$= \begin{vmatrix} A_{11} & A_{12} \\ A_{21} & A_{22} \end{vmatrix} + \begin{vmatrix} A_{11} & A_{13} \\ A_{31} & A_{33} \end{vmatrix} + \begin{vmatrix} A_{22} & A_{23} \\ A_{32} & A_{33} \end{vmatrix}$$

$$a_2 = \gamma_1 + \gamma_2 + \gamma_3 = A_{11} + A_{22} + A_{33}$$

The necessary and sufficient conditions for the numerical stability are

$$F(1) = 1 - a_2 + a_1 - a_0 \geqslant 0 \tag{30a}$$

$$F(-1) = -1 - a_2 - a_1 - a_0 \leqslant 0 \tag{30b}$$

$$|a_0| \leqslant 1 \tag{30c}$$

$$|a_0^2 - 1| \geqslant |a_0 a_2 - a_1| \tag{30d}$$

3.1. Explicit Newmark method

When the explicit Newmark method is adopted for the dynamic analysis of a SDOF structure, the coefficients of the characteristic equation (29) are

$$a_0 = 0 \tag{31a}$$

$$a_1 = 1 + \frac{\kappa}{2} - \delta\kappa - \beta \tag{31b}$$

$$a_2 = 2 - \delta\kappa - \frac{\kappa}{2} - \beta \tag{31c}$$

According to Equation (30), the necessary and sufficient conditions for unconditional stability are

$$\delta \geqslant \frac{1}{2} - \frac{\beta}{\kappa} \tag{32a}$$

$$\delta\kappa + \beta \leqslant 2 \tag{32b}$$

If $\delta = \frac{1}{2} - \beta/\kappa$ is chosen, the criterion for stability becomes $\kappa \leqslant 4$, or equivalently

$$\frac{\Delta t}{T_0} \leqslant \frac{1}{\pi}[\sqrt{1 - 3\zeta^2} + \zeta] \approx \frac{1}{\pi}(1 + \zeta) \tag{33}$$

3.2. OS method

When the OS method is adopted for the dynamic analysis of a SDOF structure, the coefficients of the characteristic equation (29) are

$$a_0 = 0 \tag{34a}$$

$$a_1 = 1 + (\tfrac{1}{2} - \delta)\kappa - \beta \tag{34b}$$

$$a_2 = 2 - (\delta + \tfrac{1}{2})\kappa - \beta \tag{34c}$$

According to Equation (30), the necessary and sufficient conditions for unconditional stability are

$$\delta \geqslant \frac{1}{2} - \frac{\beta}{\kappa} \tag{35a}$$

$$\delta\kappa + \beta \leqslant 2 \tag{35b}$$

If $\delta = \frac{1}{2} - \beta/\kappa$ and $\alpha = \frac{1}{4}$ are chosen, the criterion for stability becomes $\kappa \leqslant 4$, or equivalently

$$\frac{\Delta t}{T_0} \leqslant \frac{1}{\pi}\left(\frac{\zeta + \sqrt{1-\theta+(4\theta-3)\zeta^2}}{1-\theta}\right) \approx \frac{1}{\pi}\left(\frac{1}{\sqrt{1-\theta}} + \frac{\zeta}{1-\theta}\right), \quad 0 \leqslant \theta \leqslant 1 \tag{36a}$$

$$\frac{\Delta t}{T_0} \leqslant \infty, \quad \theta \geqslant 1. \tag{36b}$$

Disregarding damping, Equation (36a) is simplified as $\Delta t/T_0 \leqslant 1/\pi\sqrt{1-\theta}$. If $\theta \geqslant 1$ as depicted in Equation (36b), that is, the actual stiffness is less than the initial stiffness (softening type), the OS method is unconditionally stable regardless of the value of $\Delta t/T_0$, as confirmed by Nakashima *et al.* [8]

3.3. OS–SSP method

When the OS–SSP method is adopted for the dynamic analysis of an undamped SDOF structure, the effective system matrix can be derived as

$$\mathbf{A} = \begin{bmatrix} \mathbf{A}_{11} & \mathbf{A}_{12} & \mathbf{A}_{13} \\ \mathbf{A}_{21} & \mathbf{A}_{22} & \mathbf{A}_{23} \\ \mathbf{A}_{31} & \mathbf{A}_{32} & \mathbf{A}_{33} \end{bmatrix} \tag{37}$$

where

$$\mathbf{A}_{11} = \cos(\sqrt{\theta}\omega_0\Delta t) + \frac{(1-\theta)}{\theta}\cos(\sqrt{\theta}\omega_0\Delta t)\left[\frac{\sin(\sqrt{\theta}\omega_0\Delta t)}{\sqrt{\theta}\omega_0\Delta t} - 1\right]$$

$$\mathbf{A}_{12} = \frac{\sin(\sqrt{\theta}\omega_0\Delta t)}{\sqrt{\theta}\omega_0\Delta t} + \frac{(1-\theta)}{\theta}\frac{\sin(\sqrt{\theta}\omega_0\Delta t)}{\sqrt{\theta}\omega_0\Delta t}\left[\frac{\sin(\sqrt{\theta}\omega_0\Delta t)}{\sqrt{\theta}\omega_0\Delta t} - 1\right]$$

$$\mathbf{A}_{13} = -\left(\frac{1-\theta}{\theta}\right)^2\cos(\sqrt{\theta}\omega_0\Delta t) + \left(\frac{1-\theta}{\theta}\right)^2\frac{\sin(\sqrt{\theta}\omega_0\Delta t)}{\sqrt{\theta}\omega_0\Delta t}(1+\cos(\sqrt{\theta}\omega_0\Delta t))$$
$$-\left(\frac{1-\theta}{\theta}\right)^2\frac{\sin^2(\sqrt{\theta}\omega_0\Delta t)}{(\sqrt{\theta}\omega_0\Delta t)^2} + \left(\frac{1-\theta}{\theta}\right)$$

$$\times \cos(\sqrt{\theta}\omega_0\Delta t) - \left(\frac{1-\theta}{\theta}\right)\frac{\sin(\sqrt{\theta}\omega_0\Delta t)}{\sqrt{\theta}\omega_0\Delta t}$$

$$\mathbf{A}_{21} = -\sqrt{\theta}\omega_0\Delta t\,\sin(\sqrt{\theta}\omega_0\Delta t) + \left(\frac{1-\theta}{\theta}\right)$$

$$\times \cos(\sqrt{\theta}\omega_0\Delta t)[\cos(\sqrt{\theta}\omega_0\Delta t) - 1]$$

$$\mathbf{A}_{22} = \cos(\sqrt{\theta}\omega_0\Delta t) + \left(\frac{1-\theta}{\theta}\right)\frac{\sin(\sqrt{\theta}\omega_0\Delta t)}{\sqrt{\theta}\omega_0\Delta t}[\cos(\sqrt{\theta}\omega_0\Delta t) - 1]$$

$$\mathbf{A}_{23} = \left(\frac{1-\theta}{\theta}\right)^2 \cos(\sqrt{\theta}\omega_0\Delta t)(\cos(\sqrt{\theta}\omega_0\Delta t) - 1) + \left(\frac{1-\theta}{\theta}\right)^2 \frac{\sin(\sqrt{\theta}\omega_0\Delta t)}{\sqrt{\theta}\omega_0\Delta t}$$

$$\times (1 - \cos(\sqrt{\theta}\omega_0\Delta t)) + \left(\frac{1-\theta}{\theta}\right)(1 - \cos(\sqrt{\theta}\omega_0\Delta t))$$

$$- \left(\frac{1-\theta}{\theta}\right)\sqrt{\theta}\omega_0\Delta t\,\sin(\sqrt{\theta}\omega_0\Delta t)$$

$$\mathbf{A}_{31} = \cos(\sqrt{\theta}\omega_0\Delta t)$$

$$\mathbf{A}_{32} = \frac{\sin(\sqrt{\theta}\omega_0\Delta t)}{\sqrt{\theta}\omega_0\Delta t}$$

$$\mathbf{A}_{33} = \left(\frac{1-\theta}{\theta}\right)\left[\cos(\sqrt{\theta}\omega_0\Delta t) - \frac{\sin(\sqrt{\theta}\omega_0\Delta t)}{\sqrt{\theta}\omega_0\Delta t}\right]$$

and θ is defined by Equation (12). The coefficients of the characteristic equation (29) are

$$a_0 = 0 \tag{38a}$$

$$a_1 = 1 \tag{38b}$$

$$a_2 = 2\cos(\sqrt{\theta}\omega_0\Delta t) + \frac{2\sin(\sqrt{\theta}\omega_0\Delta t)}{\sqrt{\theta}\omega_0\Delta t}\left(1 - \frac{1}{\theta}\right)(1 - \cos(\sqrt{\theta}\omega_0\Delta t)) \tag{38c}$$

According to Equation (30), the necessary and sufficient conditions for unconditional stability are

$$-\cot^2\left(\frac{\sqrt{\theta}\omega_0\Delta t}{2}\right) \leqslant \frac{\sin(\sqrt{\theta}\omega_0\Delta t)}{\sqrt{\theta}\omega_0\Delta t}\left(1 - \frac{1}{\theta}\right) \leqslant 1 \tag{39}$$

The stability limit obtained numerically from Equation (39) for the proposed OS–SSP method depends on θ, as depicted in Figure 1, while the stability limit curve for the OS method is comparatively presented.

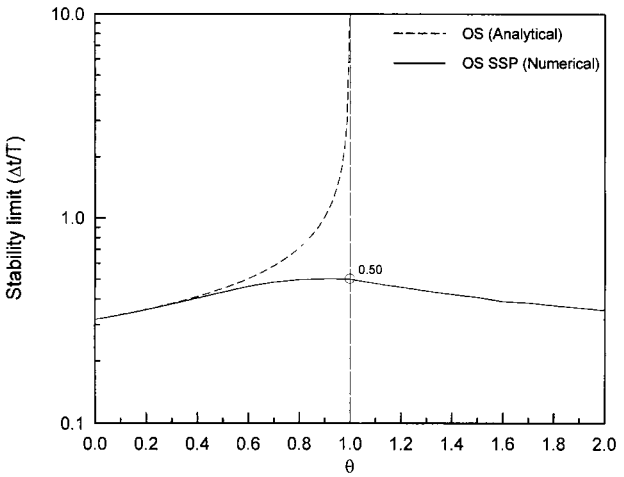

Figure 1. Scope of numerical stability for the OS–SSP method.

4. ACCURACY ANALYSIS OF NUMERICAL METHODS

Eigenvalue, frequency- and time-domain analysis can evaluate the accuracy of the numerical methods. The eigenvalues of the effective system matrices can extract the system parameters including the natural frequencies and damping ratios. Verification via an eigenvalue analysis of the numerical procedures reveals that the natural frequencies and damping ratios of the structures might not be conserved. Verification via a frequency-domain analysis of the numerical procedures also verifies that the location and magnitude of the peaks of the frequency response functions (that only contain steady-state responses) might not be conserved. By time-domain analysis, the accuracy of the numerical methods can be obtained by comparing the response time histories (containing both the transient and the steady-state responses). Only a time-domain analysis can assess non-linear behaviours.

4.1. Accuracy in eigenvalue analysis

The modulus ρ_i and phase angle ϑ_i of the eigenvalue γ_i of the effective system matrix, **A**, can extract the effective natural frequency f_i' and the effective damping ratio ζ_i' as

$$f_i' = \frac{\sqrt{(\ln \rho_i)^2 + \vartheta_i^2}}{\Delta t} \tag{40a}$$

$$\zeta_i' = -\frac{\ln \rho_i}{\sqrt{(\ln \rho_i)^2 + \vartheta_i^2}} \tag{40b}$$

Figure 2 depicts the effective frequencies with respect to the sampling ratio $\Delta t/T_0$. An analysis employing the explicit Newmark method tends to overestimate the vibration frequency with the $\Delta t/T_0$ increased, within the stability limit at $\Delta t/T_0 = 1/\pi$. An analysis by the OS method (with

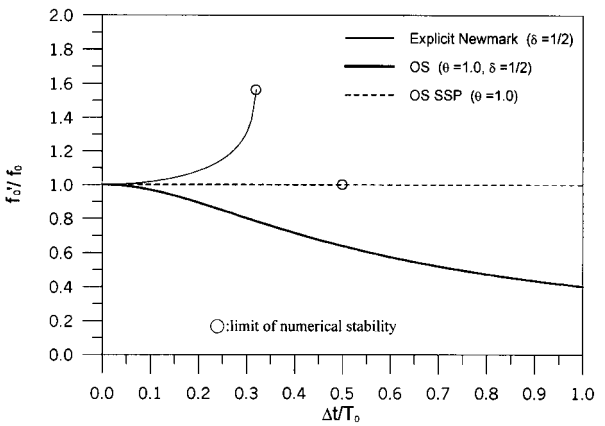

Figure 2. Accuracy of natural frequency.

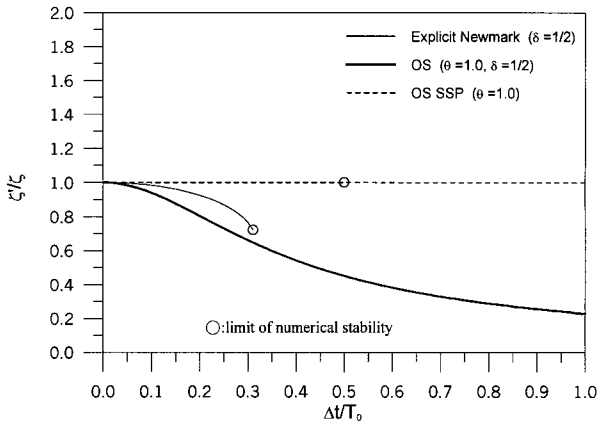

Figure 3. Accuracy of damping ratio.

$\theta = 1$ for elastic structures) tends to underestimate the vibration frequency with the $\Delta t/T_0$ increased. Conversely, an analysis by the OS–SSP method (with $\theta = 1$ for elastic structures) conserves the vibration frequency within the stability limit at $\Delta t/T_0 = 0.5$ without distortion.

Figure 3 illustrates the effective damping ratios with respect to the sampling ratio, $\Delta t/T_0$, where a damping ratio of 0.01 is assumed for the structures. The explicit Newmark (with $\delta = \frac{1}{2}$) and OS (with $\delta = \frac{1}{2}$, $\alpha = \frac{1}{4}$) methods tend to underestimate the damping ratio as $\Delta t/T_0$ increases (within the corresponding stability limits), while the OS–SSP method sufficiently conserves the damping ratio within the stability limit ($\Delta t/T_0 = 0.5$). Although both the explicit Newmark and OS (with $\delta = \frac{1}{2}$) methods are not numerically dissipative for undamped systems [2, 12], they do not conserve the damping properties for damped structures.

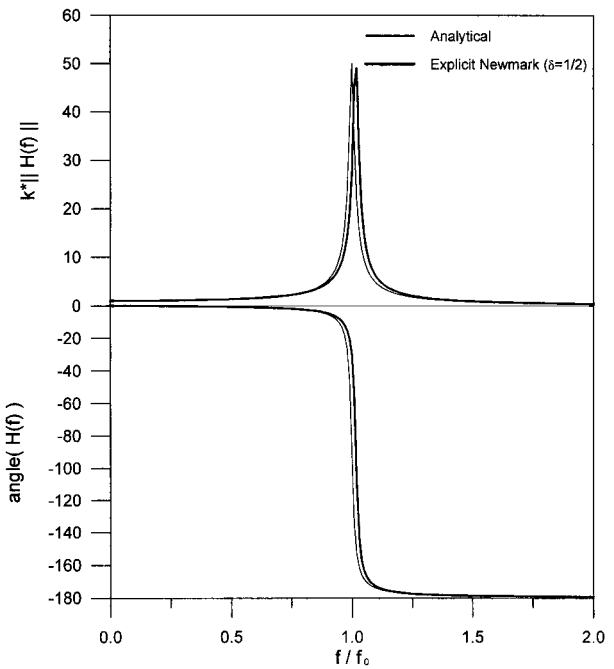

Figure 4. Accuracy of displacement frequency response function by explicit Newmark method ($\Delta t/T_0 = 0.1,\ \xi = 0.01$).

4.2. *Accuracy in frequency-domain analysis*

After taking discrete-time Fourier transformation for the difference equations (7), (11) and (28), the structural responses $\bar{\mathbf{z}}_k$ and external disturbance w_k are related in the frequency domain by

$$\bar{\mathbf{z}}(f) = \mathbf{H}(f) w(f) \tag{41}$$

where $\bar{\mathbf{z}}(f)$ and $w(f)$ are the discrete-time Fourier transformations of structural responses $\bar{\mathbf{z}}_k$ and external disturbance w_k, respectively, and $\mathbf{H}(f)$ is the frequency response function. The frequency response functions for the explicit Newmark method and the OS method are

$$\mathbf{H}(f) = (\mathrm{e}^{\mathrm{j}2\pi f \Delta t}\mathbf{I} - \mathbf{A})^{-1}(\mathrm{e}^{\mathrm{j}2\pi f \Delta t}\bar{\mathbf{E}}) \tag{42}$$

and for the OS–SSP method,

$$\mathbf{H}(f) = (\mathrm{e}^{\mathrm{j}2\pi f \Delta t}\mathbf{I} - \mathbf{A})^{-1}(\bar{\mathbf{E}}_0 + \mathrm{e}^{\mathrm{j}2\pi f \Delta t}\bar{\mathbf{E}}_1) \tag{43}$$

If the value of $\Delta t/T_0$ is sufficiently small (for example $\Delta t/T_0 \leqslant 0.05$), as revealed from eigenvalue analysis (see Figures 2 and 3), sufficient accuracy in any of the numerical method discussed can be achieved. However, the sampling ratio may easily exceed 0.05 for structures containing high-frequency responses. An accuracy analysis of the numerical methods is further evaluated with $\Delta t/T_0 = 0.1$ employing the frequency-domain analysis.

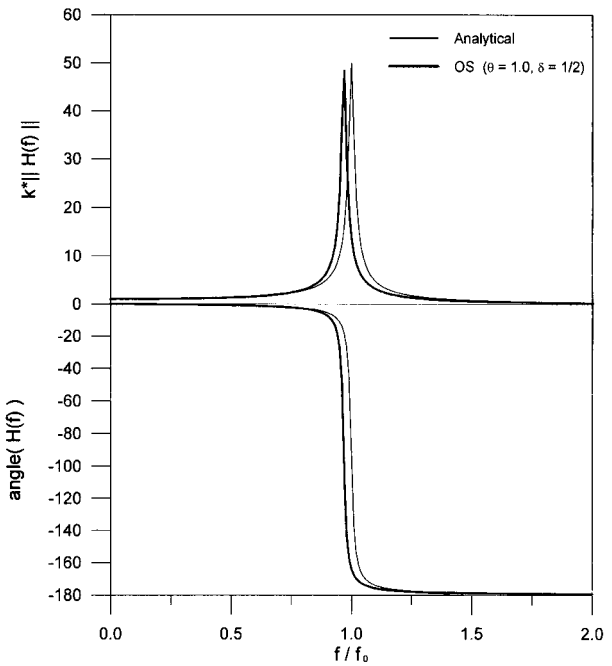

Figure 5. Accuracy of displacement frequency response function by OS method ($\Delta t/T_0 = 0.1$, $\xi = 0.01$).

Employing the explicit Newmark method, the peak of the frequency response remains relatively unchanged in magnitude and shifted rightward (Figure 4). Employing the OS method (with $\theta = 1$ for linear structures), the peak of the frequency response remains relatively unchanged in magnitude and shifted leftward (Figure 5). Both methods illustrate a significant frequency distortion for frequency ratios (f/f_0 nearby 1), however, no distortion for frequency ratios beyond 1.5 and below 0.5. Furthermore, the OS–SSP method (with $\theta = 1$ and $\Delta t/T_0 = 0.1$) indicates no distortion of the frequency response function, regardless of the frequency ratios (Figure 6), confirming a complete conservation of the structure's dynamic characteristics.

4.3. Accuracy in time-domain analysis

The eigenvalue analysis and the frequency-domain analysis are only applicable for linear elastic systems, while the time-domain analysis is valid for both linear elastic and non-linear systems. The accuracy properties of the numerical methods are examined employing a time-domain analysis for both linear and non-linear cases next.

4.3.1. Linear case. Considering an external load

$$w(t) = a \sin 2\pi f t \tag{44}$$

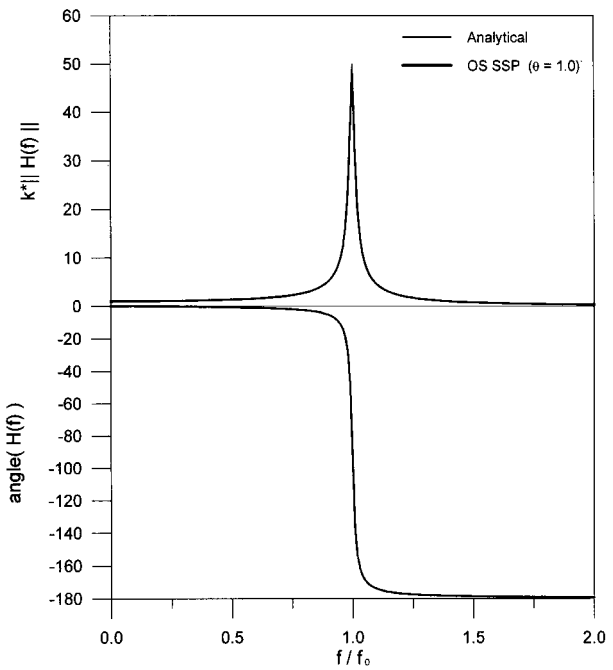

Figure 6. Accuracy of displacement frequency response function by OS–SSP method ($\Delta t/T_0 = 0.1$, $\xi = 0.01$).

where f and a are, respectively, the frequency and amplitude of the external load. The numerical solutions are obtained recursively from the difference equations (7), (11) and (28) with an integration time step $\Delta t = 0.1T_0$.

The structural responses from the numerical and exact solutions are compared in Figures 7–9 and correspond to the frequency ratio (f/f_0) between the external load and the structure of 0.5, 1.0 and 1.5, respectively. The OS–SSP method achieved an exceptional correspondence between the numerical and exact solutions, regardless of the frequency ratio. However, serious discrepancies within the numerical solutions employed by both the explicit Newmark and OS methods were observed when compared with the exact solution. This might not be anticipated except in the case of $f/f_0 = 1$, as revealed in the frequency response functions (Figures 4 and 5) where the distortion is prominent only when $f/f_0 = 1$ (approximately). The frequency response functions contain only steady-state responses. Therefore, the prediction errors by the explicit Newmark and OS methods for the cases of $f/f_0 = 0.5$ and 1.5 are primarily attributed to the transient responses. When a damping ratio of only 1 per cent is applied, the transient responses decay gradually. These results confirm the outstanding ability of the OS–SSP method to preserve both high fidelity transient and steady-state responses.

4.3.2. Non-linear case. Pseudodynamic tests are most valuable when evaluating the inelastic behaviour of seismic structures. To verify the adequacy of the on-line integration algorithms for non-linear structures, accuracy analysis was conducted for a SDOF inelastic structure whose

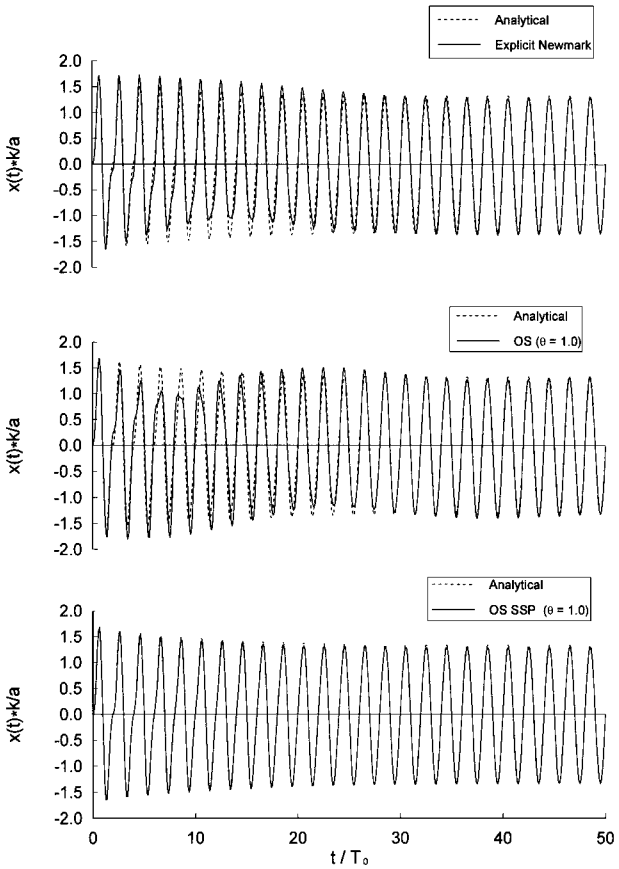

Figure 7. Accuracy of structural displacement ($\Delta t/T_0 = 0.1,\ \xi = 0.01,\ f/f_0 = 0.5$).

restoring force was represented by Wen's model [13] as

$$R(t) = vK_0x(t) + (1 - v)K_0q(t,\dot{x}) \tag{45}$$

where K_0 is the initial stiffness, x and $\dot{x}$ are, respectively, the displacement and the velocity of the structure, v is the ratio of the post-yielding stiffness to the initial stiffness and q is the hysteretic restoring deformation governed by

$$\dot{q} = \eta\dot{x} - \beta|\dot{x}||q|^{n-1}q - \varepsilon\dot{x}|q|^n \tag{46}$$

where η, β, ε and n are parameters determining the shape of the hysteresis loop (chosen in this example as $\eta = 2$, $\beta = 0.75$, $\varepsilon = 0.25$ and $n = 1$). The mass and the initial stiffness of the structure were chosen so that its fundamental period, T_0, before yielding is 0.4 s and stiffness ratio of $v = 0.5$ and damping ratio equaled 2 per cent. The sinusoidal external load represented by Equation (44) with $f/f_0 = 1$ is employed as the excitation, and the integration time interval Δt equaled

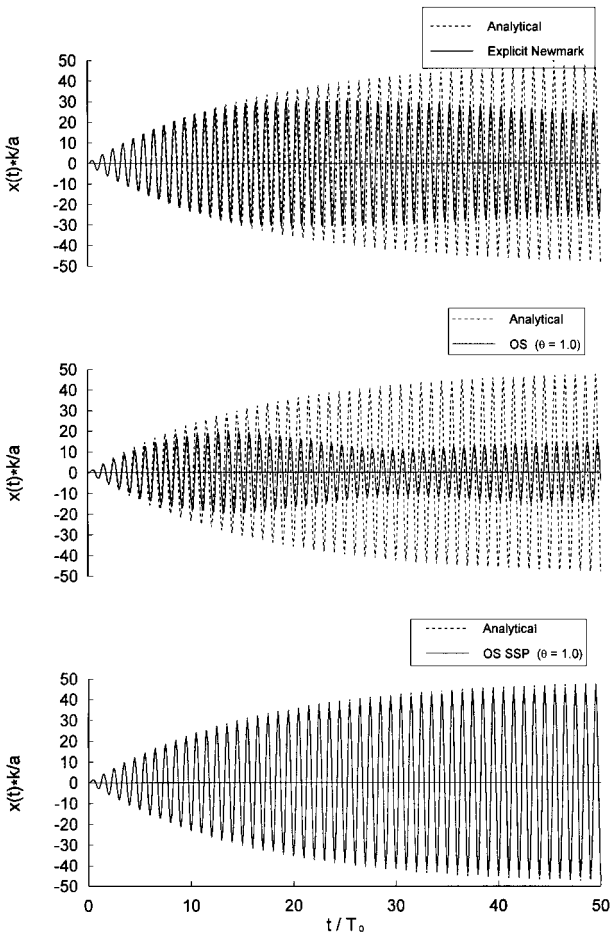

Figure 8. Accuracy of structural displacement ($\Delta t/T_0 = 0.1,\ \xi = 0.01,\ f/f_0 = 1.0$).

0.02 s such that $\Delta t/T_0 = 0.05$. Since no analytical solution existed for this nonlinear problem, the 'exact' solution was obtained by using the original state-space procedure (which cannot be used for direct pseudodynamic testing) with $\Delta t = 0.001$ s and an iterative pseudo-force corrective procedure to assure desirable precision. The accuracy of the nonlinear analysis employing the integration methods, OS–SSP and OS, with respect to the 'exact' solution was appraised by the error percentage defined as

$$Err = \frac{\sqrt{\sum_{i=1}^{N}(\bar{x}_i - x_i)^2}}{\sqrt{\sum_{i=1}^{N}(x_i)^2}} \times 100 \text{ per cent} \tag{47}$$

where x_i is the 'exact' solution at the ith time instant, $\bar{x}_i$ is the predicted solution at the ith time instant by one of the aforementioned integration algorithms and N is the total number of data.

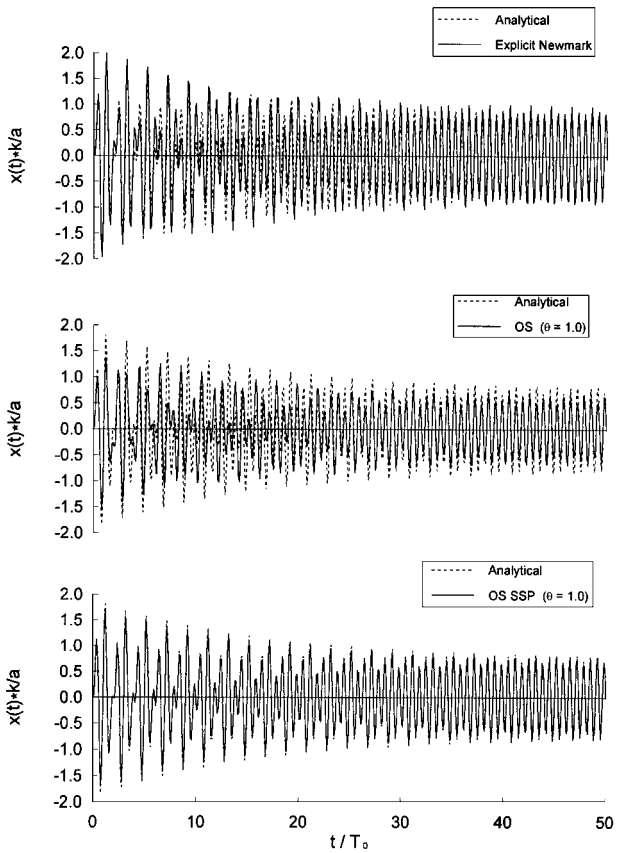

Figure 9. Accuracy of structural displacement ($\Delta t/T_0 = 0.1,\ \xi = 0.01,\ f/f_0 = 1.5$).

The displacement time history and the hysteresis of restoring force by the OS and the OS–SSP methods are illustrated in Figures 10 and 11, respectively. The OS–SSP method reveals a significant correlation between the numerical and 'exact' solutions. An error percentage of 2.3 per cent in displacement and 2.2 per cent in restoring force (within the course of 10 s) was achieved, as compared to the OS method where the error percentage of 23.5 per cent in displacement and 22.6 per cent in restoring force was estimated. The OS–SSP method, an implicit algorithm, with a one-step correction of the response calculation is comparable to the original SSP algorithm in terms of numerical accuracy, while adaptive to pseudodynamic testing.

5. CONCLUSIONS

Both the explicit Newmark and OS method commonly adopted for the pseudodynamic testing are based on the Newmark method. This article presents the OS–SSP method via an integration of the state-space procedure with Nakashima's operator-splitting concept. Numerical stability criteria

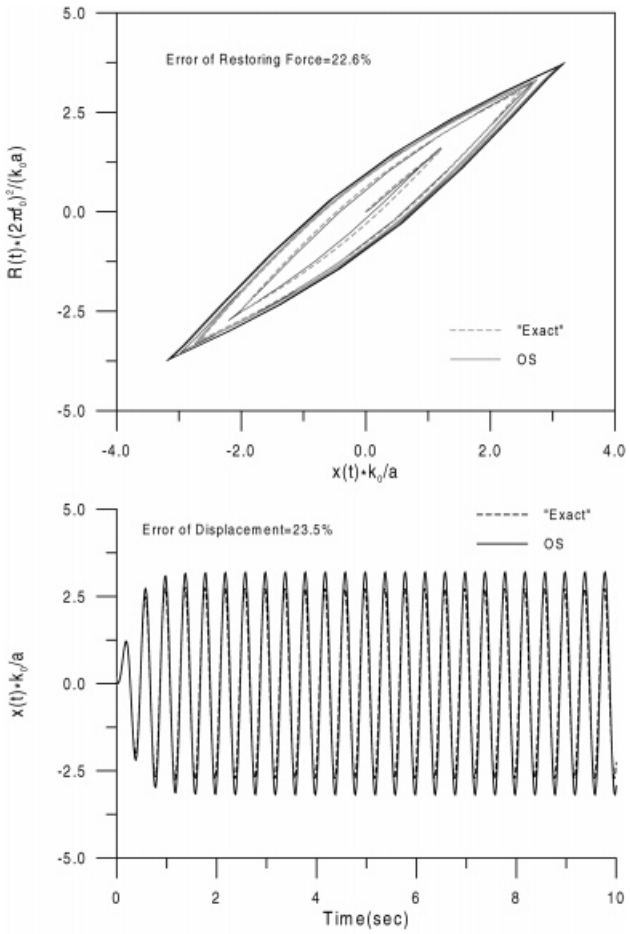

Figure 10. (a) Hysteresis of the inelastic structure by OS method. (b) Displacement of the inelastic structure by OS method ($\delta = \frac{1}{2}$, $\Delta t/T_0 = 0.05$, $\xi = 0.02$, $f/f_0 = 1.0$).

of the proposed algorithm in addition to the explicit Newmark and OS methods were determined. Moreover, an accuracy assessment was extensively explored via an eigenvalue, frequency- and time-domain analysis of linear and non-linear structures. Although the OS method was unconditionally stable for $\theta \geqslant 1$, it is inaccurate when $\Delta t/T_0 \geqslant 0.05$. The explicit Newmark method contains the worst stability characteristic, which makes it unfavourable for an analysis of structures with high-frequency responses, although it proves more accurate than the OS method within the stability range. Whereas the OS–SSP method is conditionally stable with a stability bound of $\Delta t/T_0 = 0.5$ for $\theta = 1$, it exhibits the most accurate characteristic within the stability range, as demonstrated by a consistent eigenvalue, frequency- and time-domain analysis. Therefore, the OS–SSP method is more desirable for pseudodynamic testing as long as the stability criterion ($\Delta t/T \leqslant 0.5$) is ensured for every vibration mode involved.

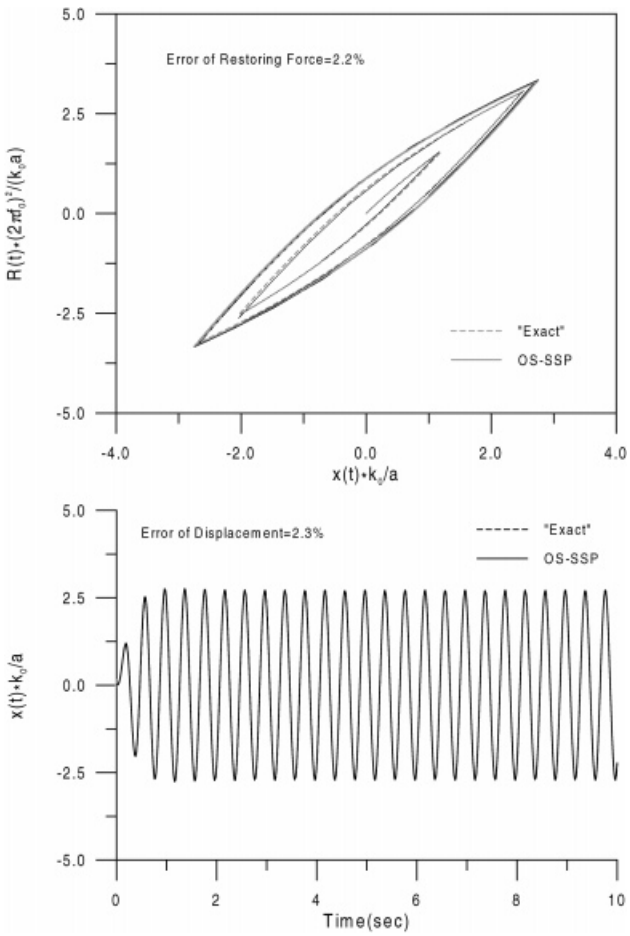

Figure 11. (a) Hysteresis of the inelastic structure by OS–SSP method. (b) Displacement of the inelastic structure by OS–SSP method ($\Delta t/T_0 = 0.05,\ \xi = 0.02,\ f/f_0 = 1.0$).

ACKNOWLEDGEMENTS

The authors would like to thank the National Science Council of the Republic of China under Grant no. NSC 87-2211-E009-028. The authors also would like to thank Dr L.L. Chung, National Center for Research on Earthquake Engineering, Taiwan, R.O.C., for his valuable discussions.

REFERENCES

1. Takanashi K, Udagawa K, Tanaka H. Earthquake response analysis of steel frames by computer-actuator on-line system. *Proceedings of the 5th Japan Earthquake Engineering Symposium*, November 1978; 1321–1328.
2. Shing PB, Mahin SA. Pseudodynamic test method for seismic performance evaluation: theory and implementation. *Report No. UCB/EERC-84/01*, Earthquake Engineering Research Center, University of California, Berkeley, CA, 1984.
3. Mahin SA, Shing PB. Pseudodynamic method for seismic testing. *Journal of Structural Engineering*, ASCE 1985; **111**(7): 1482–1501.

4. Mahin SA, Shing PB. Computational aspects of a seismic performance test method using on-line computer control. *Earthquake Engineering and Structural Dynamics* 1985; **13**: 507–526.
5. Mahin SA, Shing PB. Cumulative experimental errors in pseudodynamic tests. *Earthquake Engineering and Structural Dynamics* 1987; **15**: 409–424.
6. Mahin SA, Shing PB. Experimental error propagation in pseudodynamic testing. *Report No. UCB/EERC-83/12*, Earthquake Engineering Research Center, University of California, Berkeley, CA, 1983.
7. Thewalt CR, Mahin SA. Hybrid solution techniques for generalized pseudodynamic testing. *Report No. UCB/EERC-87-09*, Earthquake Engineering Research Center, University of California, Berkeley, CA, 1987.
8. Nakashima M, Kaminosono T, Ishida M, Ando K. Integration techniques for substructure pseudodynamic test. *Proceedings of 4th U.S. National Conference on Earthquake Engineering*, Palm Springs, CA, 1990; **2**: 515–524.
9. Lopez-Almansa F, Harbat AH, Rodellar J. SSP algorithm for linear and nonlinear dynamic response simulation. *International Journal for Numerical Methods in Engineering* 1988; **26**: 2687–2706.
10. Chung LL, Wang YP, Yang CS. Stability and accuracy of numerical analysis for structural dynamics. *Structural Engineering* 1996; **11**(4): 55–66 (in Chinese).
11. Newmark NM. A method of computation for structural dynamics. *Journal of Engineering Mechanics Division*, ASCE 1959; **85**(EM3): 67–94.
12. Hans M. Hilber, Thomas JR, Hughes, Robert L. Taylor. Improved numerical dissipation for time integration algorithm in structure dynamics. *Earthquake Engineering and Structural Dynamics* 1977; **5**: 283–292.
13. Sues RH, Mau ST, Wen YK. System identification of degrading hysteretic restoring forces. *Journal of Engineering Mechanics*, ASCE 1988; **114**(5): 833–846.

